Diagnosis and Treatment Monitoring of Port-Wine Stain Using LED-Based Photoacoustics: Theoretical Aspects and First In-Human Clinical Pilot Study

Qian Cheng, Menglu Qian, Xiuli Wang, Haonan Zhang, Peiru Wang, Long Wen, Jing Pan, Ya Gao, Shiying Wu, Mengjiao Zhang, Yingna Chen, Naoto Sato, and Xueding Wang

Abstract Port-wine stain (PWS) is categorized as a benign capillary vascular malformation, which is difficult to cure. In general, PWS appears on the face, but it can affect other areas of the body too. The affected skin surface may thicken slightly and develop an irregular, pebbled surface in adulthood. PWS's cosmetic appearance causes substantial mental stress for the patients. Currently, characterization and treatment evaluation of PWS are generally conducted using physical examination and using imaging tools like digital camera, ultrasound imaging, dermoscopy, and tristimulus colorimeters. All these commonly used imaging techniques do not offer enough imaging depth and contrast required for the accurate evaluation of PWS. In this clinical pilot study, we demonstrated for the first time that LED-based photoacoustics can be used as a point-of-care tool for clinical evaluation and PDT-treatment monitoring of PWS disease.

Haonan Zhang, Peiru Wang, Long Wen, Jing Pan, Ya Gao, Shiying Wu, Mengjiao Zhang, Yingna Chen are contributed equally to this work.

Q. Cheng (✉) · M. L. Qian · H. N. Zhang · J. Pan · Y. Gao · S. Y. Wu · M. J. Zhang · Y. N. Chen
Institute of Acoustics, School of Physics Science and Engineering, Tongji University, Shanghai, China
e-mail: q.cheng@tongji.edu.cn

X. L. Wang · P. R. Wang · L. Wen
Department of Dermatology and Venereology, Shanghai Skin Diseases Hospital, Shanghai, China

N. Sato
Research and Development Department, CYBERDYNE, INC., Tsukuba, Japan

X. D. Wang
Department of Biomedical Engineering, University of Michigan, Ann Arbor, MI, USA

M. Kuniyil Ajith Singh (ed.), *LED-Based Photoacoustic Imaging*,
Progress in Optical Science and Photonics 7,
https://doi.org/10.1007/978-981-15-3984-8_15

1 Introduction

Skin diseases, such as port-wine stain (PWS) can be diagnosed and treated using techniques like photoacoustic imaging (PAI) [1–3], photodynamic therapy (PDT) and acoustic dynamic therapy (ADT) because the lesions are located at the superficial skin layer.

PWS is a discoloration of human skin caused by a vascular anomaly (i.e., capillary malformation in the skin). In the past years, several techniques have been developed for characterization and treatment evaluation of PWS. In current dermatology clinical practice of China, physicians diagnose and evaluate the status of PWS dominantly based on subjective observation. The primary assisting tools used in the evaluation process of PWS include digital camera (DC), high-frequency ultrasound, Dermoscopy, and Tristimulus colorimeters (VISIA-CR™ system). Each of them has some limitations. Optical methods working in the ballistic regime, such as dermoscopy and VISIA, do not have sufficient penetration to cover the entire scale of PWS. High-frequency ultrasound, although with better imaging depth, does not offer sufficient contrast to differentiate PWS and healthy skin tissue.

The emerging photoacoustic (PA) imaging technology is capable of mapping the optical absorption contrast in deep biological tissue with excellent ultrasonic resolution. Combining the advantages of US imaging and fluorescence imaging, PA imaging offers great potential to offer a new way for the evaluation of PWS, quantitatively.

2 Theory

The human skin is mainly composed of three layers: epidermis, dermis, and hypodermis (Fig. 1). The epidermis is divided into two sub-layers: The stratum corneum (~10 μm thickness) with high lipids and low water content and living epidermis (~80 μm thickness) containing melanosomes for light absorption and scattering. The dermis (~2 mm thickness) has two sub-layers too: The papillary dermis and the reticular dermis, which contains two vascular plexuses, i.e., upper and deep blood plexuses in the upper and lower reticular dermis. The thickness of hypodermis is around 3 mm [4, 5].

The thickness d, light absorption coefficient η, and optical depth (ηd) of each skin layer at 840 and 532 nm are shown in Table 1 [2, 4, 6]. The optical depth of the dermis layer is the largest and contributes most to the optical absorption of the whole skin.

Especially for 840 nm, the light absorption coefficients of upper and deep blood plexuses are much larger than those of other layers, meaning that the change of the blood plexuses thickness has more effect on the total optical absorption. While not only is the epidermis thin, it also absorbs very little light. On the other hand, although the hypodermis and muscle layers are relatively thick, their absorption is much less than that of the dermis.

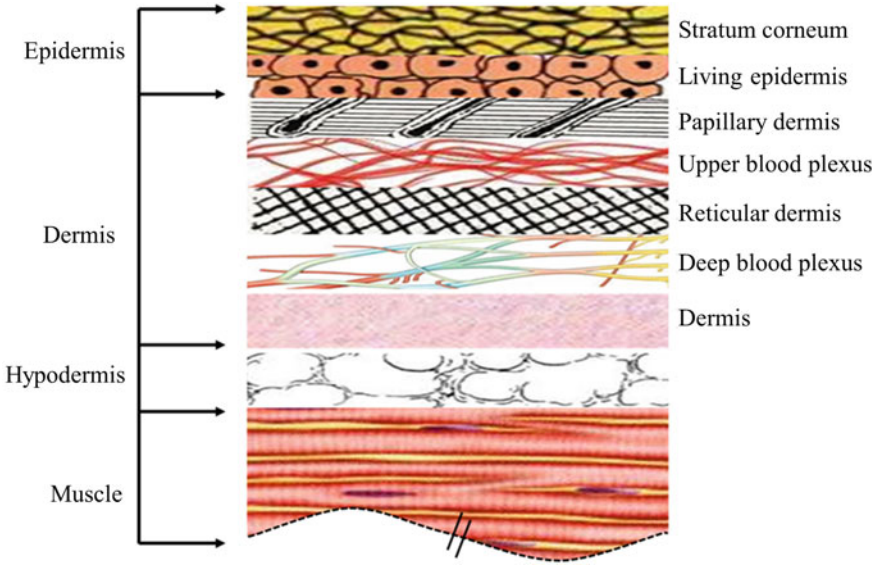

Fig. 1 Schematic of the multilayered skin

Table 1 Thickness, light absorption coefficients and optical depths of the normal skin [4, 6] and PWS [2] at 840 and 532 nm

Layers		d (mm)	$\lambda = 840$ nm		$\lambda = 532$ nm	
			η (mm^{-1})	$\eta \cdot d$	η (mm^{-1})	$\eta \cdot d$
Epidermis	Stratum corneum	0.01	0.00091	0.010	4.0	0.36
	Living epidermis	0.08	0.13		4.0	
Dermis	Papillary dermis	0.1	0.105	0.23	0.5	2.34
	Upper blood plexus	0.08	0.15875		2.45	
	Reticular dermis	1.50	0.105		0.5	
	Deep blood plexus	0.07	0.4443		18.1	
	Dermis	0.16	0.105		0.5	
Hypodermis		3.0	0.009	0.027	0.4778	1.43
Muscle tissues		3.0	0.029	0.087	0.1366	0.41
PWS (upper blood plexus)		0.1 ~ 1.5	0.15875	0.016 ~ 0.24	2.5	0.25 ~ 3.75

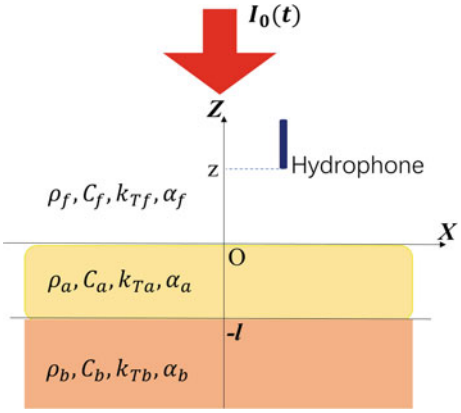

Fig. 2 Theoretical model for photoacoustic detection of skin tissue

PWS is a benign neoplasia formed by hyperplasia and dilatation of postcapillary venules throughout the epidermis and dermis of the skin. The thickness of lesion is usually about 0.1–1.5 mm, and its light absorption coefficient is similar to that of upper capillary plexuses, which causes the light absorption of skin in visible and near-infrared bands to increase significantly.

The light penetration depths $\mu_\eta(1/\bar{\eta})$ of the lesion at 840 and 532 nm are estimated at around 6.3 mm and 0.41 mm, respectively. Comprehensively considering the optical attenuation and imaging depth, it is evident that 840 nm is more suitable for PWS detection than 532 nm.

Therefore, we approximately treated the light absorption layer (lesions) as composed of the epidermis and the dermis. The hypodermis was treated with weak light absorption and the muscle tissue were took as the backing tissue without light absorption. Hence, the three layers of transparent liquid (coupling layer)—light absorption tissue (lesions)—backing tissue formed the physical model for PA signal excitation and detection (Fig. 2).

2.1 Temperature Field

A pulsed plane-wave laser beam with light intensity $I_0(t)$, wavelength λ, and pulse width τ_L is incident perpendicularly on the skin surface after passing through a transparent coupling layer f (liquid) [7]. Skin tissue is composed of two layers. The upper layer a is lesion with the thickness l, the density ρ_a, the specific heat capacity C_{Ta}, the thermal conductivity κ_{Ta}, the thermal diffusivity $\alpha_{Ta} = \kappa_{Ta}/\rho_a C_{Ta}$, and light absorption coefficient $\eta(\lambda)$, which absorbs light energy and form a heat source distributing along the depth z. The thermal power density of the heat source is,

$$g(z,t) = \eta I(z,t) = \eta I_0(t) e^{\eta z}. \quad (-l < z < 0) \tag{1.1}$$

The second layer is a semi-infinite transparent medium b, whose density, specific heat capacity, thermal conductivity, and thermal diffusivity are ρ_b, C_{Tb}, κ_{Tb}, and α_{Tb}. The heat source in medium a heats the adjacent medium b and liquid layer f through heat conduction. The PA signal is formed by the thermoelastic signal of medium a, and the thermal expansion of liquid layer f. This PA signal can be received by the acoustic probe being placed at a distance 'Z' away from the interface of layer a and f in the liquid layer. When the detector scans along x-axis (or using an ultrasound array probe), the photoacoustic images of different components or structures in the tissue can be obtained together with the ultrasound images.

The temperature fields $T_a(z,t)$, $T_b(z,t)$, and $T_f(z,t)$ in media a, b and f respectively satisfy the heat conduction equation:

$$\frac{\partial^2}{\partial z^2}T_a(z,t) - \frac{1}{\alpha_{Ta}}\frac{\partial}{\partial t}T_a(z,t) = -\frac{g(z,t)}{k_{Ta}} = -\frac{\eta}{k_{Ta}}I_0(t)e^{\eta z}, \quad (0 \geq z > -l) \tag{1.2}$$

$$\frac{\partial^2}{\partial z^2}T_b(z,t) - \frac{1}{\alpha_{Tb}}\frac{\partial}{\partial t}T_b(z,t) = 0, \quad (-l \geq z > -\infty) \tag{1.3}$$

$$\frac{\partial^2}{\partial z^2}T_f(z,t) - \frac{1}{\alpha_{Tf}}\frac{\partial}{\partial t}T_f(z,t) = 0 \quad (z > 0) \tag{1.4}$$

Here, $\alpha_{Tj} = \kappa_{Tj}/\rho_j C_{Tj}$ and κ_{Tj} are the thermal diffusivity and conductivity of medium j (=a, b, f), respectively. ρ_j and C_{Tj} are the density, specific heat capacity accordingly. The Initial conditions at $t = 0$,

$$T_a(z,0) = T_b(z,0) = T_f(z,0) = T_\infty = 0, \tag{1.5a}$$

$$\frac{\partial}{\partial t}T_a(z,0) = \frac{\partial}{\partial t}T_b(z,0) = \frac{\partial}{\partial t}T_f(z,0) = 0, \tag{1.5b}$$

And the boundary conditions at $Z = -l$ and $Z = 0$,

$$T_b(-l,t) = T_a(-l,t), \tag{1.6a}$$

$$T_a(0,t) = T_f(0,t), \tag{1.6b}$$

$$k_{Tb}\frac{\partial}{\partial z}T_b(-l,t) = k_{Ta}\frac{\partial}{\partial z}T_a(-l,t), \tag{1.6c}$$

$$k_{Ta}\frac{\partial}{\partial z}T_a(0,t) = k_{Tf}\frac{\partial}{\partial z}T_f(0,t). \tag{1.6d}$$

The Laplace transform of heat conduction equations:

$$\frac{\partial^2}{\partial z^2}T_a(z,s) - \sigma_a^2 T_a(z,s) = -\frac{\eta}{k_{Ta}}I_0(s)e^{\eta z}, \quad (0 \geq z > -l) \tag{1.7a}$$

$$\frac{\partial^2}{\partial z^2} T_b(z,s) - \sigma_b^2 T_b(z,s) = 0, \quad (-l \geq z > -\infty) \tag{1.7b}$$

$$\frac{\partial^2}{\partial z^2} T_f(z,s) - \sigma_f^2 T_f(z,s) = 0, \quad (z > 0) \tag{1.7c}$$

Here, $\sigma_j^2 = s/\alpha_{Tj}$, $j = a, b, f$.
And the Laplace transform of boundary conditions at $Z = -l$ and $Z = 0$,

$$T_a(-l,s) = T_b(-l,s), \tag{1.8a}$$

$$T_a(0,s) = T_f(0,s), \tag{1.8b}$$

$$k_{Ta} \frac{\partial}{\partial z} T_a(-l,s) = k_{Tb} \frac{\partial}{\partial z} T_b(-l,s), \tag{1.8c}$$

$$k_{Ta} \frac{\partial}{\partial z} T_a(0,s) = k_{Tf} \frac{\partial}{\partial z} T_f(0,s), \tag{1.8d}$$

The general solution of Eq. (1.6a) is

$$T_a^h(z,s) = A(s)e^{\sigma_a z} + B(s)e^{-\sigma_a z}.$$

Assume the particular solution of Eq. (1.6a) is

$$T_a^*(z,s) = -M(s)I_0(s)e^{\eta z},$$

and substitute it to Eq. (1.6a) to obtain

$$-M(s)I_0(s)e^{\eta z}\left(\eta^2 - \sigma_a^2\right) = -\frac{\eta}{k_{Ta}} I_0(s)e^{\eta z}.$$

Then we can solve the particular solution coefficient

$$M(s) = \frac{\eta}{k_{Ta}\left(\eta^2 - \sigma_a^2\right)}, \tag{1.9}$$

So, the Laplace transform solution of temperature field in medium a is

$$T_a(z,s) = A(s)e^{\sigma_a z} + B(s)e^{-\sigma_a z} - M(s)I_0(s)e^{\eta z}. \quad (0 \geq z > -l) \tag{1.10a}$$

And the Laplace transform solutions of temperature field in medium b and f are

$$T_b(z,s) = D(s)e^{\sigma_b(z+l)}, \quad (-l \geq z > -\infty) \tag{1.10b}$$

$$T_f(z,s) = F(s)e^{-\sigma_f z}, \quad (z > 0) \tag{1.10c}$$

Substitute Eq. (1.10a)–(1.10c) into Eq. (1.8a)–(1.8d), the simultaneous equations of coefficients $A(s)$, $B(s)$, $C(s)$ and $D(s)$ can be obtained as follows,

$$\begin{aligned}
&A(s) + B(s) - F(s) = M(s)I_0(s),\\
&A(s) - B(s) + \xi F(s) = \gamma M(s)I_0(s),\\
&A(s)e^{-\sigma_a l} + B(s)e^{\sigma_a l} - D(s) = M(s)I_0(s)e^{-\eta l},\\
&A(s)e^{-\sigma_a l} - B(s)e^{\sigma_a l} - \chi D(s) = \gamma M(s)I_0(s)e^{-\eta l}.
\end{aligned} \tag{1.11}$$

Here,

$$\xi = \frac{k_{Tf}\sigma_f}{k_{Ta}\sigma_a}, \quad \chi = \frac{k_{Tb}\sigma_b}{k_{Ta}\sigma_a}, \quad \gamma = \frac{\eta}{\sigma_a}. \tag{1.11a}$$

From the coefficient determinant,

$$\Delta = \begin{vmatrix} 1 & 1 & 0 & -1 \\ 1 & -1 & 0 & \xi \\ e^{-\sigma_a l} & e^{\sigma_a l} & -1 & 0 \\ e^{-\sigma_a l} & -e^{\sigma_a l} & -\chi & 0 \end{vmatrix} = e^{-\sigma_a l}(1-\chi)(1-\xi) - e^{\sigma_a l}(1+\chi)(1+\xi),$$

$$\Delta_A = M(s)I_0(s)\begin{vmatrix} 1 & 1 & 0 & -1 \\ r & -1 & 0 & \xi \\ e^{-\eta l} & e^{\sigma_a l} & -1 & 0 \\ \gamma e^{-\eta l} & -e^{\sigma_a l} & -\chi & 0 \end{vmatrix},$$

$$\Delta_B = M(s)I_0(s)\begin{vmatrix} 1 & 1 & 0 & -1 \\ 1 & \gamma & 0 & \xi \\ e^{-\sigma_a l} & e^{-\eta l} & -1 & 0 \\ e^{-\sigma_a l} & \gamma e^{-\eta l} & -\chi & 0 \end{vmatrix},$$

$$\Delta_D = M(s)I_0(s)\begin{vmatrix} 1 & 1 & 1 & -1 \\ 1 & -1 & \gamma & \xi \\ e^{-\sigma_a l} & e^{\sigma_a l} & e^{-\eta l} & 0 \\ e^{-\sigma_a l} & -e^{\sigma_a l} & \gamma e^{-\eta l} & 0 \end{vmatrix},$$

$$\Delta_F = M(s)I_0(s)\begin{vmatrix} 1 & 1 & 0 & 1 \\ 1 & -1 & 0 & \gamma \\ e^{-\sigma_a l} & e^{\sigma_a l} & -1 & e^{-\eta l} \\ e^{-\sigma_a l} & -e^{\sigma_a l} & -\chi & \gamma e^{-\eta l} \end{vmatrix},$$

$$\Delta_A = M(s)I_0(s)\left[(1-\xi)(\gamma-\chi)e^{-\eta l} - (\gamma+\xi)(1+\chi)e^{\sigma_a l}\right],$$

$$\Delta_B = M(s)I_0(s)\left[(1+\xi)(\gamma-\chi)e^{-\eta l} - (\gamma+\xi)(1-\chi)e^{-\sigma_a l}\right],$$

$$\Delta_D = M(s)I_0(s)\left\{\left[(1+\gamma)(1+\xi)e^{\sigma_a l} - (1-\gamma)(1-\xi)e^{-\sigma_a l}\right]e^{-\eta l} - 2(\gamma+\xi)\right\},$$

$$\Delta_F = M(s)I_0(s)\big[(1+\chi)(1-\gamma)e^{\sigma_a l} - (1+\gamma)(1-\chi)e^{-\sigma_a l} + 2(\gamma-\chi)e^{-\eta l}\big].$$

We get the solution of each coefficient,

$$A(s) = \frac{\Delta_A}{\Delta} = \frac{\big[(1-\xi)(\gamma-\chi)e^{-\eta l} - (\gamma+\xi)(1+\chi)e^{\sigma_a l}\big]}{(1-\xi)(1-\chi)e^{-\sigma_a l} - (1+\xi)(1+\chi)e^{\sigma_a l}} M(s)I_0(s), \quad (1.12a)$$

$$B(s) = \frac{\Delta_B}{\Delta} = \frac{\big[(1+\xi)(\gamma-\chi)e^{-\eta l} - (\gamma+\xi)(1-\chi)e^{-\sigma_a l}\big]}{(1-\xi)(1-\chi)e^{-\sigma_a l} - (1+\xi)(1+\chi)e^{\sigma_a l}} M(s)I_0(s), \quad (1.12b)$$

$$D(s) = \frac{\Delta_D}{\Delta} = \frac{\Big\{\Big[(1+\gamma)(1+\xi)e^{\sigma_a l} - (1-\gamma)(1-\xi)e^{-\sigma_a l}\Big]e^{-\eta l} - 2(\gamma+\xi)\Big\}}{(1-\xi)(1-\chi)e^{-\sigma_a l} - (1+\xi)(1+\chi)e^{\sigma_a l}} M(s)I_0(s), \quad (1.12c)$$

$$F(s) = \frac{\Delta_F}{\Delta} = \frac{\big[(1-\gamma)(1+\chi)e^{\sigma_a l} - (1+\gamma)(1-\chi)e^{-\sigma_a l} + 2(\gamma-\chi)e^{-\eta l}\big]}{(1-\xi)(1-\chi)e^{-\sigma_a l} - (1+\xi)(1+\chi)e^{\sigma_a l}} M(s)I_0(s). \quad (1.12d)$$

Equations (1.10) and (1.12) show that the temperature field in each layer is related to the incident laser pulse power, the absorbed light energy by medium a, and the thermophysical properties of each layer of the medium. By using the Laplace transform solution of the temperature field, the displacement field and stress field in the media *a, b* and *f* can be solved by the thermoelastic equations of the solid and liquid media, then the PA signal at position Z can be deduced.

2.2 Displacement Field in Media and Photoacoustic Signal in Liquid

One-dimensional thermoelastic equation and constitutive equation along the z direction in isotropic biological tissue *a* (Fig. 2) are:

$$(\lambda_a + 2\mu_a)\frac{\partial^2 u_a}{\partial z^2} - (3\lambda_a + 2\mu_a)\beta_{Ta}\frac{\partial T_a}{\partial z} = \rho_a \frac{\partial^2 u_a}{\partial t^2},$$

$$\tau_{zza} = (\lambda_a + 2\mu_a)\frac{\partial u_a}{\partial z} - (3\lambda_a + 2\mu_a)\beta_{Ta}T_a,$$

from which it can be derived that:

$$\frac{\partial^2 u_a}{\partial z^2} - \frac{1}{c_a^2}\frac{\partial^2 u_a}{\partial t^2} = G_a \frac{\partial T_a}{\partial z}, \quad (2.1a)$$

$$\tau_{zza} = \rho_a c_a^2 \left[\frac{\partial u_a}{\partial z} - G_a T_a\right], \quad (2.1b)$$

$$c_a^2 = \frac{\lambda_a + 2\mu_a}{\rho_a}, \quad G_a = \beta_{Ta}\frac{(3\lambda_a + 2\mu_a)}{(\lambda_a + 2\mu_a)}. \quad (2.1c)$$

Similarly, one-dimensional thermoelastic equation and constitutive equation of biological tissue b (Fig. 2) are as follows:

$$\frac{\partial^2 u_b}{\partial z^2} - \frac{1}{c_b^2}\frac{\partial^2 u_b}{\partial t^2} = G_b \frac{\partial T_b}{\partial z}, \tag{2.2a}$$

$$\tau_{zzb} = \rho_b c_b^2 \left[\frac{\partial u_b}{\partial z} - G_b T_b\right], \tag{2.2b}$$

$$c_b^2 = \frac{\lambda_b + 2\mu_b}{\rho_b}, \quad G_b = \beta_{Tb}\frac{(3\lambda_b + 2\mu_b)}{(\lambda_b + 2\mu_b)}. \tag{2.2c}$$

Here, c_j is speed of longitudinal wave of medium j, G_j is thermoelastic coefficient of medium j, β_{Tj} is coefficient of linear expansion of medium j, λ_j and μ_j are Lamé elastic constants of medium j ($j = a, b$).

Acoustic wave equation in liquid f,

$$\rho_f \frac{\partial^2 u_f}{\partial t^2} = -\frac{\partial}{\partial z} p(z, t). \tag{2.3}$$

One-dimensional state equation of liquid,

$$-p(z, t) = B_f \frac{\partial u_f(z, t)}{\partial z} - B_f \beta T_f(z, t) \tag{2.3a}$$

From the derivative of Eq. (2.3a) with respect to z and substitute into Eq. (2.3), the thermoelastic equation describing liquid particle displacement can be obtained,

$$\rho_f \frac{\partial^2 u_f}{\partial t^2} = B_f \frac{\partial^2 u_f(z, t)}{\partial z^2} - B_f \beta \frac{\partial}{\partial z} T_f(z, t),$$

Or

$$\frac{\partial^2 u_f(z, t)}{\partial z^2} - \frac{1}{c_f^2}\frac{\partial^2 u_f(z, t)}{\partial t^2} = \beta \frac{\partial}{\partial z} T_f(z, t), \tag{2.4}$$

Here, β is the volume thermal expansion coefficient of liquid, ρ_f is the density of liquid, B_f is the volume elasticity coefficient of liquid, and c_f is the speed of sound of liquid,

$$c_f^2 = \frac{B_f}{\rho_f}. \tag{2.4a}$$

The initial conditions for particles motion in the three-layer media:

$$u_a(z, 0) = u_b(z, 0) = u_f(z, 0) = 0, \tag{2.5a}$$

$$\frac{\partial u_a(z,0)}{\partial t} = \frac{\partial u_b(z,0)}{\partial t} = \frac{\partial u_f(z,0)}{\partial t} = 0, \tag{2.5b}$$

The boundary condition are continuous displacement and continuous normal stress at the boundary $z = 0$ and $z = -l$,

$$u_a(0,t) = u_f(0,t), \quad \tau_{zza}(0,t) = -p(0,t), \tag{2.6a}$$

$$u_a(-l,t) = u_b(-l,t), \quad \tau_{zza}(-l,t) = \tau_{zzb}(-l,t). \tag{2.6b}$$

The Laplace transform of thermoelastic displacement Eqs. (2.1), (2.2), (2.4) and constitutive Eqs. (2.1a), (2.2a), (2.3a),

$$\frac{\partial^2 u_a(s,z)}{\partial z^2} - \frac{s^2}{c_a^2} u_a(s,z) = G_a \frac{\partial T_a(s,z)}{\partial z}, \quad (-l < z < 0) \tag{2.7a}$$

$$\frac{\partial^2 u_b(s,z)}{\partial z^2} - \frac{s^2}{c_b^2} u_b(s,z) = G_b \frac{\partial T_b(s,z)}{\partial z}, \quad (z < -l) \tag{2.7b}$$

$$\frac{\partial^2 u_f(s,z)}{\partial z^2} - \frac{s^2}{c_f^2} u_f(s,z) = \beta \frac{\partial T_f(s,z)}{\partial z}, \quad (z > 0) \tag{2.7c}$$

$$\tau_{zza}(s,z) = \rho_a c_a^2 \left[\frac{\partial u_a(s,z)}{\partial z} - G_a T_a(s,z) \right], \tag{2.8a}$$

$$\tau_{zzb}(\mathrm{s},\mathrm{z}) = \rho_b c_b^2 \left[\frac{\partial u_b(s,z)}{\partial z} - G_b T_b(s,z) \right], \tag{2.8b}$$

$$p(s,z) = -\rho_f c_f^2 \left[\frac{\partial u_f(s,z)}{\partial z} - \beta T_f(s,z) \right]. \tag{2.8c}$$

Substitute Laplace transform solution (1.10) of temperature field into Eq. (2.7), and get:

$$\frac{\partial^2 u_a(s,z)}{\partial z^2} - \frac{s^2}{c_a^2} u_a(s,z) = G_a \left[A(s)\sigma_a e^{\sigma_a z} - B(s)\sigma_a e^{-\sigma_a z} - M(s) I_0(s) \eta e^{\eta z} \right], \tag{2.9a}$$

$$\frac{\partial^2 u_b(s,z)}{\partial z^2} - \frac{s^2}{c_b^2} u_b(s,z) = G_b D(s) \sigma_b e^{\sigma_b (z+l)}, \tag{2.9b}$$

$$\frac{\partial^2 u_f(s,z)}{\partial z^2} - \frac{s^2}{c_f^2} \frac{\partial^2 u_f(s,z)}{\partial t^2} = -\sigma_f \beta F(s) e^{-\sigma_f z}. \tag{2.9c}$$

To solve the displacement field Eq. (2.9) in the three-layer media, the particular solutions of Eq. (2.9) can be set as:

$$
\begin{aligned}
u_a^*(s,z) &= G_a\left[a(s)\sigma_a e^{\sigma_a z} - b(s)\sigma_a e^{-\sigma_a z} - m(s)I_0(s)\eta e^{\eta z}\right],\\
u_b^*(s,z) &= G_b d(s)\sigma_b e^{\sigma_b(z+l)},\\
u_f^*(s,z) &= -\sigma_f \beta f(s) e^{-\sigma_f z}.
\end{aligned} \tag{2.10}
$$

Substitute Eq. (2.10) to Eq. (2.9) and determine coefficients $a(s), b(s), m(s), d(s)$, and $f(s)$ as

$$
\begin{aligned}
&a(s)\sigma_a e^{\sigma_a z}(\sigma_a^2 - \frac{s^2}{c_a^2}) = A(s)\sigma_a e^{\sigma_a z}, \quad a(s) = \frac{A(s)}{\left(\sigma_a^2 - \frac{s^2}{c_a^2}\right)},\\
&b(s)\sigma_a e^{-\sigma_a z}\left(\sigma_a^2 - \frac{s^2}{c_a^2}\right) = B(s)\sigma_a e^{-\sigma_a z}, \quad b(s) = \frac{B(s)}{\left(\sigma_a^2 - \frac{s^2}{c_a^2}\right)},\\
&m(s)I_0(s)\eta e^{\eta z}\left(\eta^2 - \frac{s^2}{c_a^2}\right) = M(s)I_0(s)\eta e^{\eta z}, \quad m(s) = \frac{M(s)}{\left(\eta^2 - \frac{s^2}{c_a^2}\right)},\\
&\left(\sigma_b^2 - \frac{s^2}{c_b^2}\right)G_b d(s)\sigma_b e^{\sigma_b(z+l)} = G_b D(s)\sigma_b e^{\sigma_b(z+l)}, \quad d(s) = \frac{D(s)}{\left(\sigma_b^2 - \frac{s^2}{c_b^2}\right)},\\
&-\sigma_f \beta f(s) e^{-\sigma_f z}\left(\sigma_f^2 - \frac{s^2}{c_f^2}\right) = -\sigma_f \beta F(s) e^{-\sigma_f z}, \quad f(s) = \frac{F(s)}{\left(\sigma_f^2 - \frac{s^2}{c_f^2}\right)}.
\end{aligned} \tag{2.11}
$$

Suppose the homogeneous general solution of Eq. (2.9) as

$$
\begin{aligned}
u_a^h(s,z) &= a^h(s)e^{(s/c_a)z} + b^h(s)e^{-(s/c_a)z},\\
u_b^h(s,z) &= d^h(s)e^{(s/c_b)(z+l)},\\
p^h(s,z) &= f^h(s)e^{-(s/c_f)z}.
\end{aligned} \tag{2.12}
$$

Therefore, the displacement transformation solutions in media a and b and the sound pressure transformation solution in the liquid are:

$$
\begin{aligned}
u_a(s,z) &= a^h(s)e^{\left(\frac{s}{c_a}\right)z} + b^h(s)e^{-\left(\frac{s}{c_a}\right)z}\\
&\quad + G_a\left[\frac{A(s)\sigma_a}{\left(\sigma_a^2 - \frac{s^2}{c_a^2}\right)}e^{\sigma_a z} - \frac{B(s)\sigma_a}{\left(\sigma_a^2 - \frac{s^2}{c_a^2}\right)}e^{-\sigma_a z} - \frac{\eta I_0(s)M(s)}{\left(\eta^2 - \frac{s^2}{c_a^2}\right)}e^{\eta z}\right], \qquad (2.13a)\\
u_b(s,z) &= d^h(s)e^{\left(\frac{s}{c_b}\right)(z+l)} + G_b\frac{D(s)\sigma_b}{\left(\sigma_b^2 - \frac{s^2}{c_b^2}\right)}e^{\sigma_b(z+l)}, \qquad (2.13b)
\end{aligned}
$$

$$u_f(s,z) = f^h(s)e^{-(s/c_f)z} - \beta\frac{F(s)\sigma_f}{\left(\sigma_f^2 - \frac{s^2}{c_f^2}\right)}e^{-\sigma_f z}. \tag{2.13c}$$

Substitute the displacement solution (2.13) into the Laplace transform of the boundary condition:

$$\begin{aligned} &u_a(0,s) = u_f(0,s), \quad \tau_{zza}(0,s) = -p(0,s),\\ &u_a(-l,s) = u_b(-l,s), \quad \tau_{zza}(-l,s) = \tau_{zzb}(-l,s), \end{aligned}$$

and get the coefficients $a^h(s), b^h(s), d^h(s)$ and $f^h(s)$. Normal stress in biological tissue is:

$$\tau_{zzj}(\mathrm{s},\mathrm{z}) = \rho_j c_j^2\left[\frac{\partial u_j(s,z)}{\partial z} - G_j T_j(s,z)\right], \quad j = a,b, \tag{2.13d}$$

And acoustic pressure in liquid is

$$\begin{aligned} p(s,z) &= -\rho_f c_f^2\left[\frac{\partial u_f(s,z)}{\partial z} - \beta T_f(s,z)\right],\\ p(s,z) &= \left[sz_f f^h(s)e^{-(s/c_f)z} - \rho_f s^2\frac{\beta F(s)}{\left(\sigma_f^2 - \frac{s^2}{c_f^2}\right)}e^{-\sigma_f z}\right], \end{aligned} \tag{2.13e}$$

Here, $z_f = \rho_f c_f$ is acoustic impedance of the liquid.

From the boundary conditions, the linear equations of the unknown coefficients are

$$a^h(s) + b^h(s) - f^h(s) = -G_a\left[\frac{A(s)\sigma_a}{\left(\sigma_a^2 - \frac{s^2}{c_a^2}\right)} - \frac{B(s)\sigma_a}{\left(\sigma_a^2 - \frac{s^2}{c_a^2}\right)} - \frac{\eta I_0(s)M(s)}{\left(\eta^2 - \frac{s^2}{c_a^2}\right)}\right] - \beta\frac{F(s)\sigma_f}{\left(\sigma_f^2 - \frac{s^2}{c_f^2}\right)}, \tag{2.14a}$$

$$a^h(s) - b^h(s) + Z_{af} f^h(s) = Z_{af}\left(\frac{s}{c_f}\right)\frac{\beta F(s)}{\left(\sigma_f^2 - \frac{s^2}{c_f^2}\right)} - \left(\frac{s}{c_a}\right)G_a\left[\frac{A(s)+B(s)}{\left(\sigma_a^2 - \frac{s^2}{c_a^2}\right)} - \frac{I_0(s)M(s)}{\left(\eta^2 - \frac{s^2}{c_a^2}\right)}\right]. \tag{2.14b}$$

$$\begin{aligned} a^h(s)e^{-\left(\frac{s}{c_a}\right)l} - b^h(s)e^{\left(\frac{s}{c_a}\right)l} - Z_{ab}d^h(s) &= G_b Z_{ab}\left(\frac{s}{c_b}\right)\frac{D(s)}{\left(\sigma_b^2 - \frac{s^2}{c_b^2}\right)}\\ &- G_a\left(\frac{s}{c_a}\right)\left[\frac{A(s)}{(\sigma_a^2 - \frac{s^2}{c_a^2})}e^{-\sigma_a l} + \frac{B(s)}{(\sigma_a^2 - \frac{s^2}{c_a^2})}e^{\sigma_a l} - \frac{I_0(s)M(s)}{\left(\eta^2 - \frac{s^2}{c_a^2}\right)}e^{-\eta l}\right], \end{aligned} \tag{2.14c}$$

$$a^h(s)e^{-\left(\frac{s}{c_a}\right)l} + b^h(s)e^{\left(\frac{s}{c_a}\right)l} - d^h(s) = G_b\left[\frac{D(s)\sigma_b}{\left(\sigma_b^2 - \frac{s^2}{c_b^2}\right)}\right]$$

$$- G_a\left[\frac{A(s)\sigma_a}{\left(\sigma_a^2 - \frac{s^2}{c_a^2}\right)}e^{-\sigma_a l} - \frac{B(s)\sigma_a}{\left(\sigma_a^2 - \frac{s^2}{c_a^2}\right)}e^{\sigma_a l} - \frac{\eta I_0(s)M(s)}{\left(\eta^2 - \frac{s^2}{c_a^2}\right)}e^{-\eta l}\right], \tag{2.14d}$$

or

$$a^h(s) + b^h(s) - f^h(s) = N_1(s), \tag{2.14a}$$

$$a^h(s) - b^h(s) + Z_{af} f^h(s) = N_2(s), \tag{2.12b}$$

$$a^h(s)e^{-\left(\frac{s}{c_a}\right)l} - b^h(s)e^{\left(\frac{s}{c_a}\right)l} - Z_{ab}d^h(s) = N_3(s), \tag{2.14c}$$

$$a^h(s)e^{-\left(\frac{s}{c_a}\right)l} + b^h(s)e^{\left(\frac{s}{c_a}\right)l} - d^h(s) = N_4(s), \tag{2.14d}$$

Here,

$$Z_{af} = \frac{z_f}{z_a} = \left(\frac{\rho_f c_f}{\rho_a c_a}\right), \quad Z_{ab} = \left(\frac{\rho_b c_b}{\rho_a c_a}\right), \tag{2.14e}$$

where, $z_j = \rho_j c_j$ is the acoustic impedance of medium j ($j = a$, b and f). And

$$N_1(s) = -G_a\left[\frac{A(s)\sigma_a}{(\sigma_a^2 - \frac{s^2}{c_a^2})} - \frac{B(s)\sigma_a}{(\sigma_a^2 - \frac{s^2}{c_a^2})} - \frac{\eta I_0(s)M(s)}{\left(\eta^2 - \frac{s^2}{c_a^2}\right)}\right] - \beta\frac{F(s)\sigma_f}{\left(\sigma_f^2 - \frac{s^2}{c_f^2}\right)}, \tag{2.15a}$$

$$N_2(s) = Z_{af}\left(\frac{s}{c_f}\right)\frac{\beta F(s)}{\left(\sigma_f^2 - \frac{s^2}{c_f^2}\right)} - \left(\frac{s}{c_a}\right)G_a\left[\frac{A(s) + B(s)}{(\sigma_a^2 - \frac{s^2}{c_a^2})} - \frac{I_0(s)M(s)}{\left(\eta^2 - \frac{s^2}{c_a^2}\right)}\right], \tag{2.15b}$$

$$N_3(s) = Z_{ab}\left(\frac{s}{c_b}\right)G_b\frac{D(s)}{(\sigma_b^2 - \frac{s^2}{c_b^2})} - \left(\frac{s}{c_a}\right)G_a\left[\frac{A(s)}{(\sigma_a^2 - \frac{s^2}{c_a^2})}e^{-\sigma_a l} + \frac{B(s)}{(\sigma_a^2 - \frac{s^2}{c_a^2})}e^{\sigma_a l} - \frac{I_0(s)M(s)}{\left(\eta^2 - \frac{s^2}{c_a^2}\right)}e^{-\eta l}\right], \tag{2.15c}$$

$$N_4(s) = G_b\left[\frac{D(s)\sigma_b}{(\sigma_b^2 - \frac{s^2}{c_b^2})}\right]$$

$$- G_a \left[\frac{A(s)\sigma_a}{(\sigma_a^2 - \frac{s^2}{c_a^2})} e^{-\sigma_a l} - \frac{B(s)\sigma_a}{(\sigma_a^2 - \frac{s^2}{c_a^2})} e^{\sigma_a l} - \frac{\eta I_0(s) M(s)}{\left(\eta^2 - \frac{s^2}{c_a^2}\right)} e^{-\eta l} \right]. \quad (2.15d)$$

The coefficient determinant Δ and Δ_f of Eqs. (2.14a–2.14d)

$$\Delta = \begin{vmatrix} 1 & 1 & 0 & -1 \\ 1 & -1 & 0 & Z_{af} \\ e^{-\left(\frac{s}{c_a}\right)l} & -e^{\left(\frac{s}{c_a}\right)l} & -Z_{ab} & 0 \\ e^{-\left(\frac{s}{c_a}\right)l} & e^{\left(\frac{s}{c_a}\right)l} & -1 & 0 \end{vmatrix}, \quad \Delta_f = \begin{vmatrix} 1 & 1 & 0 & N_1(s) \\ 1 & -1 & 0 & N_2(s) \\ e^{-\left(\frac{s}{c_a}\right)l} & -e^{\left(\frac{s}{c_a}\right)l} & -Z_{ab} & N_3(s) \\ e^{-\left(\frac{s}{c_a}\right)l} & e^{\left(\frac{s}{c_a}\right)l} & -1 & N_4(s) \end{vmatrix},$$

So,

$$\Delta = \left[(1 + Z_{af})(1 + Z_{ab}) e^{\left(\frac{s}{c_a}\right)l} - (1 - Z_{af})(1 - Z_{ab}) e^{-\left(\frac{s}{c_a}\right)l} \right], \quad (2.16a)$$

$$\Delta_f = [N_2(s) - N_1(s)](1 + Z_{ab}) e^{\left(\frac{s}{c_a}\right)l} + [N_2(s) + N_1(s)](1 - Z_{ab}) e^{-\left(\frac{s}{c_a}\right)l} - 2N_3(s) + 2Z_{ab} N_4(s). \quad (2.16b)$$

The coefficient of the general solution of displacement field in liquid is

$$f^h(s) = \frac{\Delta_f}{\Delta} = \left\{ \frac{[N_2(s) - N_1(s)](1 + Z_{ab}) e^{\left(\frac{s}{c_a}\right)l} + [N_2(s) + N_1(s)](1 - Z_{ab}) e^{-\left(\frac{s}{c_a}\right)l} - 2N_3(s) + 2Z_{ab} N_4(s)}{\left[(1 + Z_{af})(1 + Z_{ab}) e^{\left(\frac{s}{c_a}\right)l} - (1 - Z_{af})(1 - Z_{ab}) e^{-\left(\frac{s}{c_a}\right)l} \right]} \right\}. \quad (2.17a)$$

Thus, the Laplace transform solution of the photoacoustic signal in the liquid can be obtained from Eq. (2.13e):

$$p(s, z) = \left[s z_f f^h(s) e^{-(s/c_f)z} - s^2 \frac{\rho_f \beta F(s)}{\left(\sigma_f^2 - \frac{s^2}{c_f^2}\right)} e^{-\sigma_f z} \right]. \quad (2.17b)$$

Let $s = i\omega$ in the above equation, photoacoustic signal spectrum can be expressed as,

$$p(\omega, z) = i z_f \omega f^h(\omega) e^{-ik_f z} + \rho_f \omega^2 \frac{\beta}{\left(\sigma_f^2 + k_f^2\right)} F(\omega) e^{-\sigma_f(\omega) z}], \quad k_f^2 = \frac{\omega^2}{c_f^2}. \quad (2.18a)$$

where, the acoustic displacement amplitude of liquid particle is:

$$f^h(\omega) = \left\{ \frac{\left[N_2(\omega) - N_1(\omega)\right](1+Z_{ab})e^{ika l} + \left[N_2(\omega) + N_1(\omega)\right](1-Z_{ab})e^{-ika l} - 2N_3(\omega) + 2Z_{ab}N_4(\omega)}{(1+Z_{af})(1+Z_{ab})e^{ika l} - (1-Z_{af})(1-Z_{ab})e^{-ika l}} \right\}. \tag{2.18b}$$

While

$$F(\omega) = \frac{\left[(1-\gamma)(1+\chi)e^{\sigma_a l} - (1+\gamma)(1-\chi)e^{-\sigma_a l} + 2(\gamma-\chi)e^{-\eta l}\right]}{(1-\xi)(1-\chi)e^{-\sigma_a l} - (1+\xi)(1+\chi)e^{\sigma_a l}} M(\omega) I_0(\omega). \tag{2.18c}$$

Here,

$$M(\omega) = \frac{\eta}{k_{Ta}\left(\eta^2 - \sigma_a^2\right)}, \quad \sigma_j(\omega) = (1+i)\sqrt{\frac{\omega}{2\alpha_j}} = \frac{(1+i)}{\mu_j(\omega)}, \quad (j = a, b, f)$$

Here, $\sigma_j(\omega)$ is he heat wave vector in medium j, and $\mu_j(\omega)$ is its heat diffusion length. And

$$N_1(\omega) = -\beta \frac{F(\omega)\sigma_f}{\left(\sigma_f^2 + k_f^2\right)} - G_a \left[\frac{A(\omega)\sigma_a}{(\sigma_a^2 + k_a^2)} - \frac{B(\omega)\sigma_a}{(\sigma_a^2 + k_a^2)} - \frac{\eta I_0(\omega) M(\omega)}{\left(\eta^2 + k_a^2\right)} \right], \tag{2.19a}$$

$$N_2(\omega) = i Z_{af} \frac{k_f \beta F(\omega)}{\left(\sigma_f^2 + k_f^2\right)} - i k_a G_a \left[\frac{A(\omega)}{(\sigma_a^2 + k_a^2)} + \frac{B(\omega)}{(\sigma_a^2 + k_a^2)} - \frac{I_0(\omega) M(\omega)}{\left(\eta^2 + k_a^2\right)} \right], \tag{2.19b}$$

$$\begin{aligned} N_3(\omega) = {} & i G_b Z_{ab} \frac{k_b D(\omega)}{(\sigma_b^2 + k_b^2)} \\ & - i k_a G_a \left[\frac{A(\omega)}{(\sigma_a^2 + k_a^2)} e^{-\sigma_a l} + \frac{B(\omega)}{(\sigma_a^2 + k_a^2)} e^{\sigma_a l} - \frac{I_0(\omega) M(\omega)}{\left(\eta^2 + k_a^2\right)} e^{-\eta l} \right], \end{aligned} \tag{2.19c}$$

$$N_4(\omega) = G_b \left[\frac{D(\omega)\sigma_b}{(\sigma_b^2 + k_b^2)} \right] - G_a \left[\frac{A(\omega)\sigma_a}{(\sigma_a^2 + k_a^2)} e^{-\sigma_a l} - \frac{B(\omega)\sigma_a}{(\sigma_a^2 + k_a^2)} e^{\sigma_a l} - \frac{\eta I_0(\omega) M(\omega)}{\left(\eta^2 + k_a^2\right)} e^{-\eta l} \right], \tag{2.19d}$$

$$A(\omega) = \frac{\left[(1-\xi)(\gamma-\chi)e^{-\eta l} - (\gamma+\xi)(1+\chi)e^{\sigma_a l}\right]}{(1-\xi)(1-\chi)e^{-\sigma_a l} - (1+\xi)(1+\chi)e^{\sigma_a l}} M(\omega) I_0(\omega), \tag{2.20a}$$

$$B(\omega) = \frac{\left[(1+\xi)(\gamma-\chi)e^{-\eta l} - (\gamma+\xi)(1-\chi)e^{-\sigma_a l}\right]}{(1-\xi)(1-\chi)e^{-\sigma_a l} - (1+\xi)(1+\chi)e^{\sigma_a l}} M(\omega) I_0(\omega), \tag{2.20b}$$

$$D(\omega) = \frac{\left\{\left[(1+\gamma)(1+f)e^{\sigma_a l} - (1-\gamma)(1-\xi)e^{-\sigma_a l}\right]e^{-\eta l} - 2(\gamma+\xi)\right\}}{(1-\xi)(1-\chi)e^{-\sigma_a l} - (1+\xi)(1+\chi)e^{\sigma_a l}} M(\omega) I_0(\omega), \tag{2.20c}$$

Equation (2.18) is the theoretical solution of PA signal generated by a two-layer medium (light absorbing medium/semi-infinite non-absorbing substrate) in a semi-infinite fluid. Equations (2.18)–(2.20) show that the light energy absorbed by the medium can produce a PA signal consisting of two parts, i.e. acoustic and thermal wave. It is relevant to the incident light intensity, light absorption coefficient, the thickness of medium a, thermal diffusion lengths, acoustic impedance of three kinds of medium, acoustic frequency etc. Through the measurement of PA spectrum, the mechanical and thermal properties of medium can be nondestructively tested and evaluated.

2.3 Photoacoustic Signal of PWS

PWS is a congenital abnormal proliferation of capillaries that does not resolve on its own. The lesion thickens and darkens with age. Clinically, the lesion thickness (l) will be around 0.1–3 mm. Under 840 nm wavelength, due to the difference of the capillary network density, the average light absorption coefficients of isolated lesions are different. The light penetration depth μ_η at 840 nm of capillaries is about 5–10 mm, according to the data from Table 1 $\left(\mu_\eta = 1/\bar{\eta}\right)$.

In the range of frequency from 1 to 10 MHz, the wavelength of sound wave in water is 1.5–0.15 mm, and the thermal diffusion length μ_a of skin and vasculature are around 1.04–0.33 μm and 0.286–0.090 μm when their thermal diffusivity α_{Ta} are about 6.75 $\mathrm{mm^2\,s^{-1}}$ and 0.513 $\mathrm{mm^2\,s^{-1}}$, respectively.

Therefore, for PWS, the light penetration depth μ_η is much higher than the acoustic wavelength λ_{ac} and lesions thickness l, which are higher than the thermal diffusion length μ_a. So PWS is a kind of weak light absorption and thermally "thick" sample for the wavelength 840 nm. That is:

$$\mu_\eta \gg (\lambda_{ac}, l) \gg \left(\mu_a, \mu_f\right), \text{i.e.} \eta \ll \left(k_a, k_f\right) \ll \left(\sigma_a, \sigma_{f.}\right). \tag{3.1}$$

But the low-frequency approximation of $k_a l \ll 1$ is not satisfied. So, using the formula

$$e^{\pm i k_a l} = cos(k_a l) \pm i sin(k_a l),$$

Equation (2.18b) can be rewritten as

$$f^h(\omega) = \frac{\Delta_f}{\Delta} = \frac{\left[N_2(\omega) - Z_{ab}N_1(\omega)\right]cos(k_a l) - i\left[N_1(\omega) - Z_{ab}N_2(\omega)\right]sin(k_a l) - N_3(\omega) + Z_{ab}N_4(\omega)}{(Z_{af} + Z_{ab})cos(k_a l) + i(1 + Z_{ab}Z_{af})sin(k_a l)}. \tag{3.2}$$

Here,

$$\Delta_f = \left[N_2(\omega) - Z_{ab}N_1(\omega)\right]cos(k_a l) - i\left[N_1(\omega) - Z_{ab}N_2(\omega)\right]sin(k_a l) - N_3(\omega) + Z_{ab}N_4(\omega) \tag{3.2a}$$

$$\Delta = \left(Z_{af} + Z_{ab}\right)cos(k_a l) + i\left(1 + Z_{ab}Z_{af}\right)sin(k_a l). \tag{3.2b}$$

Photoacoustic spectrum generated by light absorption of PWS in the fluid can be written as

$$p(\omega, z) \approx i z_f \omega f^h(\omega) e^{-ik_f z}, \quad k_f^2 = \frac{\omega^2}{c_f^2}. \tag{3.3}$$

Using Eq. (3.1) and

$$e^{-\eta l} \approx (1 - \eta l), \quad e^{-\sigma_a l} \approx 0,$$

Equations (2.18)–(2.20) can be written as

$$f = \frac{k_{Tf}\sigma_f}{k_{Ta}\sigma_a}, \quad b = \frac{k_{Tb}\sigma_b}{k_{Ta}\sigma_a}, \quad \sigma_j(\omega) = (1+i)\sqrt{\frac{\omega}{2\alpha_j}} = \frac{(1-i)}{\mu_j}, \quad (j = a, b, f)$$

$$Z_{af} = \frac{\rho_f c_f}{\rho_a c_a}, \quad Z_{ab} = \frac{\rho_b c_b}{\rho_a c_a}, \quad G_a = \beta_{Ta}\frac{(3\lambda_a + 2\mu_a)}{(\lambda_a + 2\mu_a)}, \quad G_b = \beta_{Tb}\frac{(3\lambda_b + 2\mu_b)}{(\lambda_b + 2\mu_b)},$$

$$r = \frac{\eta}{\sigma_a} \ll 1, \quad M(\omega) \approx -\frac{\eta}{k_{Ta}\sigma_a^2}, \tag{3.4a}$$

$$A(\omega) \approx \frac{(r+f)}{(1+f)} M(\omega) I_0(\omega) \approx \frac{f}{(1+f)} M(\omega) I_0(\omega), \tag{3.4b}$$

$$B(\omega) \approx -\frac{(r-b)(1-\eta l)}{(1+\mathrm{b})e^{\sigma_a l}} M(\omega) I_0(\omega) \approx \frac{b(1-\eta l)}{(1+\mathrm{b})e^{\sigma_a l}} M(\omega) I_0(\omega), \tag{3.4c}$$

$$D(\omega) \approx -\frac{(1+r)(1-\eta l)}{(1+\mathrm{b})} M(\omega) I_0(\omega) \approx -\frac{(1-\eta l)}{(1+\mathrm{b})} M(\omega) I_0(\omega), \tag{3.4d}$$

$$F(\omega) \approx -\frac{(1-r)}{(1+f)} M(\omega) I_0(\omega) \approx -\frac{1}{(1+f)} M(\omega) I_0(\omega), \tag{3.4e}$$

and

$$\begin{aligned} N_1(\omega) &\approx -\beta\frac{F(\omega)}{\sigma_f} - G_a\left[\frac{A(\omega)}{\sigma_a} - \frac{B(\omega)}{\sigma_a} - \frac{\eta I_0(\omega) M(\omega)}{k_a^2}\right] \\ &\approx -\beta\frac{F(\omega)}{\sigma_f} - G_a\left[\frac{A(\omega)}{\sigma_a} - \frac{\eta I_0(\omega) M(\omega)}{k_a^2}\right] \\ &\approx \left[\frac{\beta}{\sigma_f(1+f)} + \frac{\eta G_a}{k_a^2}\right] I_0(\omega) M(\omega) \approx \frac{\eta G_a}{k_a^2} I_0(\omega) M(\omega), \end{aligned} \tag{3.5a}$$

$$N_2(\omega) \approx i Z_{af}\frac{k_f \beta F(\omega)}{\sigma_f^2} - i k_a G_a\left[\frac{A(\omega)}{\sigma_a^2} + \frac{B(\omega)}{\sigma_a^2} - \frac{I_0(\omega) M(\omega)}{k_a^2}\right]$$

$$\approx iZ_{af}\frac{k_f\beta F(\omega)}{\sigma_f^2} - ik_aG_a\left[\frac{A(\omega)}{\sigma_a^2} - \frac{I_0(\omega)M(\omega)}{k_a^2}\right] \ll iN_1(\omega), \tag{3.5b}$$

$$N_3(\omega) \approx iG_bZ_{ab}\frac{k_bD(\omega)}{\sigma_b^2} - ik_aG_a\left[\frac{A(\omega)}{\sigma_a^2}e^{-\sigma_a l} + \frac{B(\omega)}{\sigma_a^2}e^{\sigma_a l} - \frac{I_0(\omega)M(\omega)}{k_a^2}(1-\eta l)\right]$$

$$\approx iG_bZ_{ab}\frac{k_bD(\omega)}{\sigma_b^2} - ik_aG_a\left[\frac{B(\omega)}{\sigma_a^2}e^{\sigma_a l} - \frac{I_0(\omega)M(\omega)}{k_a^2}(1-\eta l)\right] \ll iN_4(\omega), \tag{3.5c}$$

$$\begin{aligned} N_4(\omega) &\approx G_b\left[\frac{D(\omega)}{\sigma_b}\right] - G_a\left[\frac{A(\omega)}{\sigma_a}e^{-\sigma_a l} - \frac{B(\omega)}{\sigma_a}e^{\sigma_a l} - \frac{\eta I_0(\omega)M(\omega)}{k_a^2}(1-\eta l)\right] \\ &\approx G_b\left[\frac{D(\omega)}{\sigma_b}\right] + G_a\left[\frac{B(\omega)}{\sigma_a}e^{\sigma_a l} + \frac{\eta I_0(\omega)M(\omega)}{k_a^2}(1-\eta l)\right]. \\ &\approx (1-\eta l)\left[\frac{\eta G_a}{k_a^2} - \frac{G_b}{\sigma_b(1+\mathrm{b})}\right]I_0(\omega)M(\omega) \approx \frac{\eta(1-\eta l)G_a}{k_a^2}I_0(\omega)M(\omega). \end{aligned} \tag{3.5d}$$

So,

$$\begin{aligned} \Delta_f &\approx [N_2(\omega) - Z_{ab}N_1(\omega)]\cos(k_a l) \\ &\quad - i[N_1(\omega) - Z_{ab}N_2(\omega)]\sin(k_a l) - N_3(\omega) + Z_{ab}N_4(\omega) \\ &\approx -[Z_{ab}\cos(k_a l) + i\sin(k_a l)]N_1(\omega) + Z_{ab}N_4(\omega) \\ &\approx \{Z_{ab}[1-\eta l - \cos(k_a l)] - i\sin(k_a l)\}\frac{\eta G_a}{k_a^2}I_0(\omega)M(\omega) \end{aligned}$$

Using

$$M(\omega) \approx -\frac{\eta}{k_{Ta}\sigma_a^2}, \quad \sigma_a^2(\omega) = -\frac{i\omega}{\alpha_{Ta}}, \quad \alpha_{Ta} = \frac{k_{Ta}}{\rho_a C_{Ta}},$$

to substitute into the above equation and get:

$$\Delta_f \approx \frac{\eta^2 G_a}{i\omega k_a^2}\frac{1}{\rho_a C_{Ta}}\{Z_{ab}[1-\eta l - \cos(k_a l)] - i\sin(k_a l)\}I_0(\omega). \tag{3.6}$$

Therefore, the displacement amplitude of the fluid particle is:

$$f^h(\omega) = \frac{\Delta_f}{\Delta} \approx \frac{\eta^2 G_a}{i\omega k_a^2}\frac{1}{\rho_a C_{Ta}}\left\{\frac{Z_{ab}[1-\eta l - \cos(k_a l)] - i\sin(k_a l)}{(Z_{af}+Z_{ab})\cos(k_a l) + i(1+Z_{ab}Z_{af})\sin(k_a l)}\right\}I_0(\omega). \tag{3.7}$$

The corresponding normalized PA signal spectrum is:

$$\bar{p}(\omega, z) = i\omega z_f f^h(\omega)e^{-ik_f z}/I_0(\omega)$$

$$\bar{p}(\omega, z) \approx G_a\frac{\eta^2 z_f}{k_a^2}\frac{1}{\rho_a C_{Ta}}\left\{\frac{Z_{ab}[1-\eta l - \cos(k_a l)] - i\sin(k_a l)}{(Z_{af}+Z_{ab})\cos(k_a l) + i(1+Z_{ab}Z_{af})\sin(k_a l)}\right\}e^{-ik_f z}, \quad k_a^2 = \frac{\omega^2}{c_a^2}. \tag{3.8}$$

The results show that the PA signal of PWS is proportional to the light absorption coefficient η^2 and inversely proportional to the frequency ω^2, which is associated with the mechanical and thermal properties of lesions. Therefore, PWS can be diagnosed quantitatively with PA imaging technique.

For most patients with mild lesions, whose thickness satisfies $(k_a l) \ll 1$, so

$$\cos(k_a l) \approx 1, \quad \sin(k_a l) \approx k_a l \ll 1, \quad \eta l \ll 1.$$

Equation (3.7) can be further simplified to:

$$\bar{p}(\omega, z) \approx -G_a \frac{\eta^2 \mathrm{z}_f}{k_a^2} \frac{1}{\rho_a C_{Ta}} \left\{ \frac{\eta l \mathrm{Z}_{ab} + i(k_a l)}{(\mathrm{Z}_{af} + \mathrm{Z}_{ab}) + i(1 + \mathrm{Z}_{ab}\mathrm{Z}_{af})(k_a l)} \right\} e^{-ik_f z},$$

or

$$\bar{p}(\omega, z) \approx -G_a \frac{\mathrm{z}_f z_a}{(\mathrm{z}_f + \mathrm{z}_b)} \frac{\eta^2 l}{\rho_a C_{Ta}} \left(\eta \frac{\mathrm{z}_b}{z_a} \frac{c_a^2}{\omega^2} + i \frac{c_a}{\omega} \right) e^{-ik_f z}. \tag{3.9}$$

This suggests that the PA signal amplitude is proportional to the lesion thickness l, increases rapidly with the increase of light absorption coefficient η and reduces rapidly with the increase of frequency ω. So, it's very sensitive to the changes of capillary density in the lesion. Therefore, PA diagnosis technique is a highly sensitive detection method for PWS.

3 Clinical Pilot Study

3.1 Material & Methods

The US and PA images were acquired by an LED-based PA and US imaging system (AcousticX, CYBERDYNE, INC., Tsukuba, Japan), which has been introduced in a previous publication [8]. The LED array has 144 elements, each with a size of 1 mm × 1 mm. The four lines of 36 elements distribute on an area of 6.88 mm × 50.4 mm, providing 200 μJ pulse energy at 850-nm wavelength. Working with a pulse repetition rate of 4 kHz, extensive signal averaging can be conducted to enhance the signal-to-noise ratio (SNR). The LED-produced PA image and US image from a sample can be acquired simultaneously by this dual-modality system. A 128-element linear probe working at 9 MHz central frequency was used to acquire the PA and US images. The light from the LED array illuminated the skin with a power density of 2.6 kW/m^2, which is below the safety limit of 5.98 kW/m^2, according to the international electrotechnical commission (IEC) 6247117 [9].

A coupling water bag (Fig. 3a) is sterilized by alcohol before each imaging procedure. Figure 3b shows a typical data acquisition scene with a performer (left) and

Fig. 3 **a** Photograph of coupling water bag and imaging probe, **b** clinical imaging scene, and **c** patient positioning

a patient (right). During the imaging period, the patient is required to lie flatly on a testing bed to fully expose the PWS region of interest (ROI), as is shown in Fig. 3c. For each ROI, we choose one healthy region (HR) with the most similar anatomical condition to it (we pick the symmetric position of ROI if available) as well for one additional imaging process to perform offline data processing. Before each imaging procedure, the performer will mark the ROI, as shown in Fig. 4, with the red arrow, and the corresponding HR, as indicated by the blue arrow. The arrows' orientations indicate the right side of resulting images.

During the imaging process, the performer scans the ROI with the imaging probe, and then record all the images involved. The result with the most appropriate contrast will then be picked for data processing. The same procedure is performed for each matched HR of every ROI.

In every selected image, firstly, an empty area away from ROI is circled out for the measurement of averaged PA signal amplitude (E_{pa}), which indicates the noise level of present image that is required for signal calibration. Afterwards, the performer

Fig. 4 Photograph of a PWS patient with imaging assisting marks

observes the results of ROI and matched HR to circle out areas suspended for the incidence of PWS in the ROI and the symmetric healthy region in matched HR. The E_{pa} values of ROI and HR are then divided by the noise level, yielding to V_{tar} and V_{nor}. We define a parameter—PWS level by V_{tar}/V_{nor}, to quantitatively describe the status of each ROI. Figure 5 gives the typical comparison of ROI and HR in an adult patient.

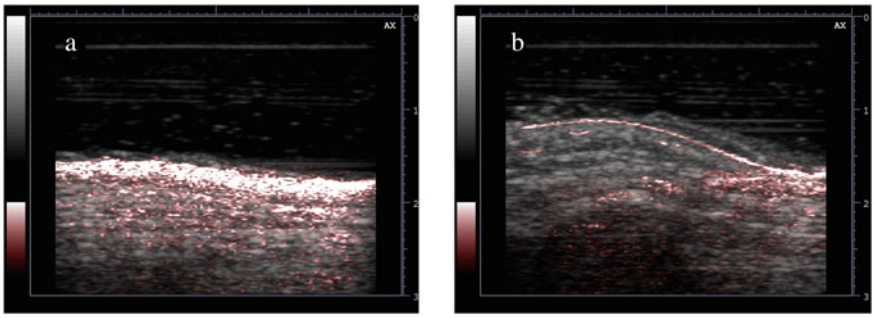

Fig. 5 Typical photoacoustic/ultrasound overlay image of **a** PWS region (ROI) and **b** control region (HR)

3.2 *Results and Discussion*

3.2.1 PA Evaluation for Various Age Groups

As a typical capillary disorder, continuous development with age is an important feature of PWS. Figure 6 shows the photograph of 3 patients, age of 4, 13 and 33 years, respectively. It is clear that the darkness and the diseased skin thickness both grow with the age of patients.

In this study, a total of 22 patients were included. The clinical evaluation for each patient given by DC, dermoscopy, and VISIA were collected, as well as the newly developed PWS level parameter acquired by the PAI system. The typical data set for one patient is shown in Fig. 7.

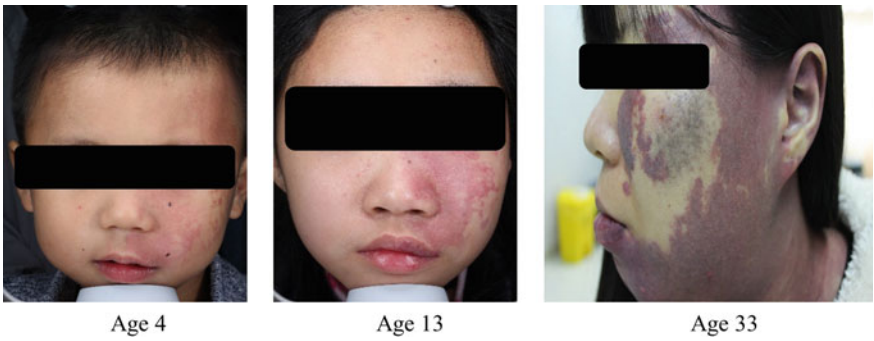

Fig. 6 Photograph of patients with various ages

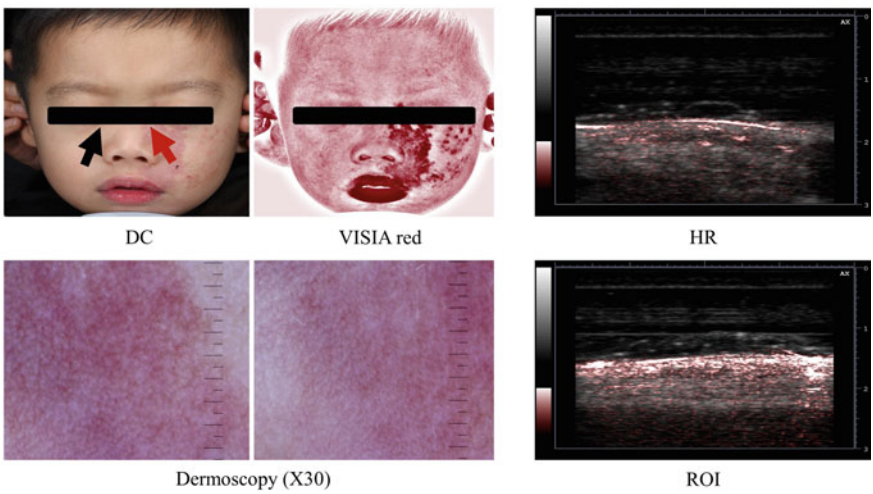

Fig. 7 Typical data set from a patient

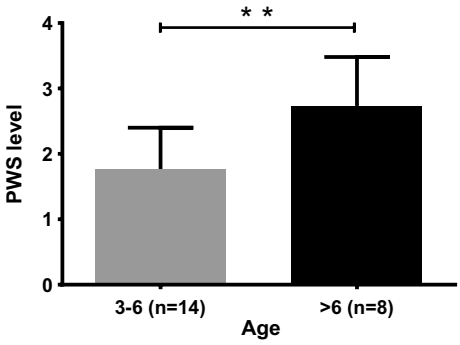

Fig. 8 PWS level comparison of the 2 groups

The enrolled 22 patients were divided into two groups, according to their ages, as 3–6 years old and above 6 years old. The PWS level comparison of the two groups is shown in Fig. 8. The mean PWS levels of 3–6 years group and >6 years group are 1.77 ± 0.63 and 2.73 ± 0.75, respectively.

The significant difference of the two different age groups correspond well with the given knowledge of PWS disease. Based on this result, the new parameter PWS level holds good potential in evaluation of PWS. To further demonstrate this point, study of dynamic monitoring of PWS before and after PDT treatment was conducted, which is detailed in next section.

3.2.2 PA Evaluation for PDT Treatment Efficacy

In current clinical practices in China, hematoporphyrin monomethyl ether photodynamic therapy (HMME-PDT) is proved to be an effective method for treating PWS [10, 11].

Two out of the 22 patients volunteered this study for dynamic PWS level monitoring, as shown in Figs. 9 and 10. The immediate reduction of PWS level corresponds to the edema instantly after the PDT treatment. At 3-day point, the PWS level of each patient shows a recovering status, or even getting worse (Fig. 9), which corresponds to the damage-repairing period that starts at that time point. The repairing period often comes with a hyperemia status, which is the reason why the PWS level gets back here. Nonetheless, after that period, the PWS level goes down steadily, and eventually gets to the 2-month endpoint.

Five out of the 22 patients volunteered for PWS level monitoring before and 2-month after PDT treatment, the result of which is shown in Fig. 11. A mean PWS level reduction of $41.08\% \pm 11.30\%$ was observed after one PDT treatment. From our results, it is clear that approximately 3–4 PDT treatments are required to completely cure the patient.

The dynamic monitoring results show the good correspondence of PWS level to the actual patient's status, and the 2-month PWS level monitor shows the efficacy of PDT treatment. Based on these results, it is clear that the PWS level parameter

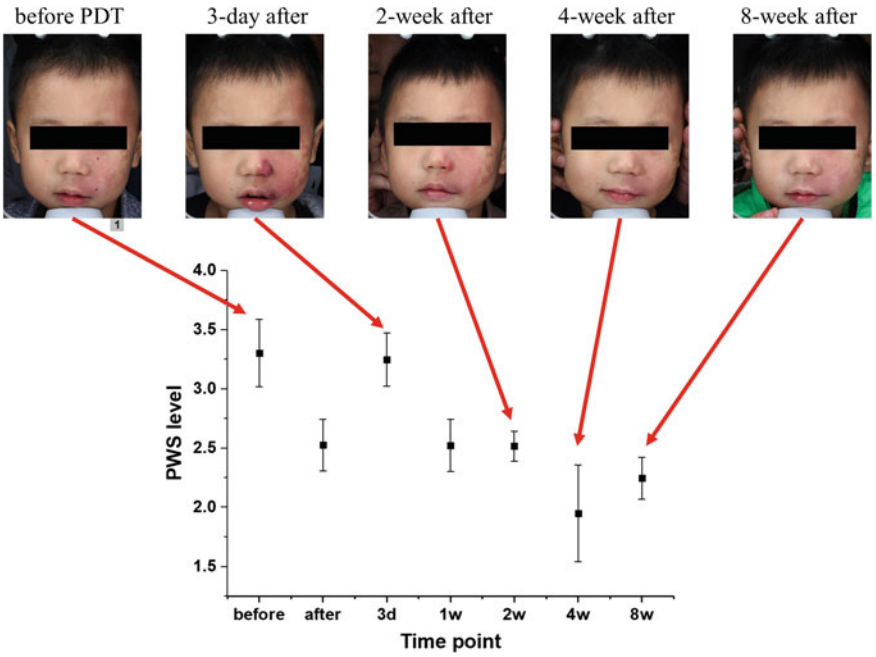

Fig. 9 Dynamic PWS level monitoring #Patient 1

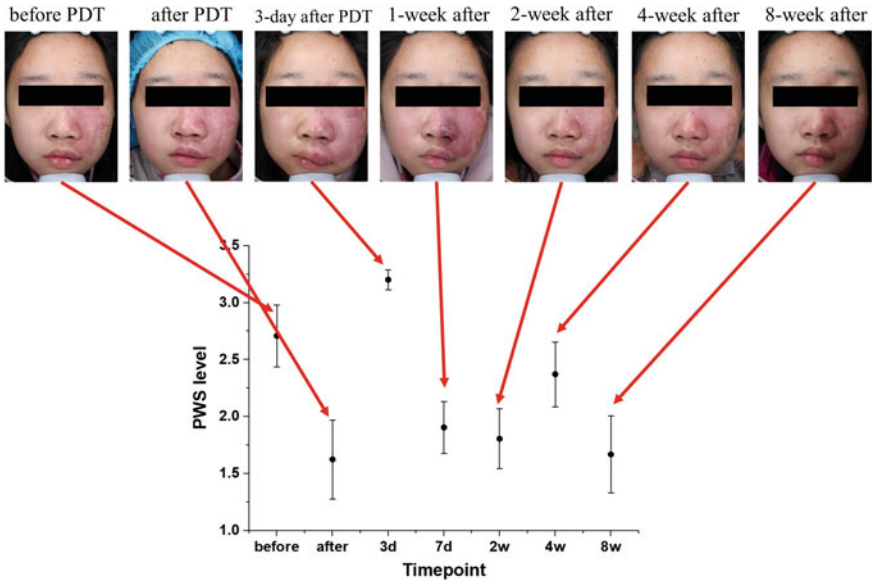

Fig. 10 Dynamic PWS level monitoring #Patient 2

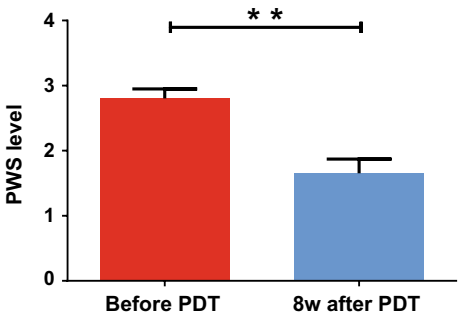

Fig. 11 2-months PWS level monitor

holds good potential to be used as a guiding tool for dose control in the treatment process of PDT. Additionally, as a quantitative tool, the PWS level of patients can be collected to serve as the source for big-data analysis as well, which will lead to a better understanding of this disease, or even other capillary disorders.

Other than mapping the hemoglobin, by combing different wavelengths that have optical absorption contrast on oxyhemoglobin and deoxyhemoglobin, the PA imaging is also capable of mapping the oxygen saturation [12, 13]. By scanning the imaging probe, it is technically feasible to perform volumetric imaging as well. In addition, for the practice of dermatology, the proposed protocol, which is already in a clinical-procedure-equivalent manner, is easily translatable to clinics.

4 Summary and Outlook

PAI has inherent advantages for vascular recognition. Firstly, compared with other biological macromolecules, hemoglobin has a very high absorption for the near-infrared light which leads to the high specificity for hemoglobin with PAI using these wavelengths. Secondly, due to the process of light-in and sound-out, the sensitivity and resolution of PAI is much higher than that of ultrasonic imaging, which makes it possible to image capillaries. But, because of the tiny size of the capillaries, traditional PA theory is no longer applicable for their quantitative diagnosis. Instead, the optical, thermal, mechanical and acoustic properties of different biological tissues need to be analyzed in the micro-scale. Meanwhile, the effects of some different parameters, such as light penetration depth, thermal diffusion length, wavelength of sound wave, and vascular size, on photoacoustic signals are very important and these are covered in the theoretical section of this chapter. This theoretical analysis can also be applied to other similar layered tissue with strong light absorption.

Current clinical results have already demonstrated the safety, functional contrast and clinic-friendly protocol of this LED-based PAI strategy. This ongoing research has already shown its great translational potential. Moreover, other than the discussed application of PWS evaluation, this imaging strategy is also potentially useful to assist doctors in assessing many other skin diseases, vascular tumor or skin carcinomas

that come with microvessels malformation or angiotelectasis, like actinic keratosis (AK), Bowen's disease (BD), superficial basal cell carcinoma (BCC), squamous cell carcinoma (SCC) and extramammary Paget's disease (EMPD). Besides, some inflammatory skin diseases, like psoriasis, are accompanied with vascular abnormity as well, which could also be a potential application. Furthermore, the application could be extended to fundus oculi lesion diagnosis, angiogenesis monitoring, and so on. We believe that PAI, as an emerging imaging strategy, would promisingly play a greater role in the early stage evaluation of a lot of diseases located in the light-accessible depth range.

5 Conclusions

PWS levels acquired using LED-based PAI holds strong potential to be a quantitative parameter for the evaluation of PWS status. We demonstrated for the first time that LED-based photoacoustics can be used as a point-of-care tool for clinical evaluation of PWS disease. Our results also give a direct indication that LED-based PAI is useful for guiding PDT-treatments.

Acknowledgements Authors gratefully acknowledge the patients who participated in this clinical study.

Ethical Approval All procedures for human subjects in this study were approved by the Ethics Committee of Shanghai Skin Disease Hospital (2019-06).

References

1. R.G.M. Kolkman, M.J. Mulder, C.P. Glade et al., Photoacoustic imaging of port-wine stains. Lasers Surg. Med. **40**, 178–182 (2008)
2. J.A. Viator, B. Choi, M. Ambrose et al., In vivo port-wine stain depth determination with a photoacoustic probe. Appl. Opt. **42**, 3215 (2003)
3. H. Zhang, J. Pan, L. Wen et al., A novel light emitting diodes based photoacoustic evaluation method for port wine stain and its clinical trial (Conference Presentation), in *Photons Plus Ultrasound: Imaging and Sensing 2019*. International Society for Optics and Photonics (2019), p. 1087807
4. J.A. Iglesias-Guitian, C. Aliaga, A. Jarabo et al., A biophysically-based model of the optical properties of skin aging. Computer Graphics Forum **34**, 45–55 (2015)
5. A. Bhowmik, R. Repaka, S.C. Mishra et al., Analysis of radiative signals from normal and malignant human skins subjected to a short-pulse laser. Int. J. Heat Mass Transf. **68**, 278–294 (2014)
6. A.N. Bashkatov, E.A. Genina, V.V. Tuchin, Optical properties of skin, subcutaneous, and muscle tissues: a review. J Innov Opt Health Sci **04**, 9–38 (2011)
7. D.L. Balageas, J.C. Krapez, P. Cielo, Pulsed photothermal modeling of layered materials. J. Appl. Phys. **59**, 348–357 (1986)

8. Y. Zhu, G. Xu, J. Yuan et al., Light Emitting Diodes based Photoacoustic Imaging and Potential Clinical Applications. *Sci Rep*; 8. Epub ahead of print December 2018. https://doi.org/10.1038/s41598-018-28131-4
9. Commission, I. E. IEC 62471: 2006 Photobiological safety of lamps and lamp systems. International Standard (2006). http://tbt.testrust.com/image/zt/123/100123_2.pdf. Accessed 26 Nov 2018
10. Y. Zhao, P. Tu, G. Zhou et al., Hemoporfin photodynamic therapy for port-wine stain: a randomized controlled trial. PLoS ONE **11**, e0156219 (2016)
11. L. Wen, Y. Zhang, L. Zhang et al., Application of different noninvasive diagnostic techniques used in HMME-PDT in the treatment of port wine stains. Photodiagn. Photodyn. Ther. **25**, 369–375 (2019)
12. X. Wang, G. Ku, X. Xie et al., Noninvasive functional photoacoustic tomography of blood-oxygen saturation in the brain, in ed. A.A. Oraevsky, L.V. Wang (San Jose, CA), p. 69
13. X. Wang, X. Xie, G. Ku et al., Noninvasive imaging of hemoglobin concentration and oxygenation in the rat brain using high-resolution photoacoustic tomography. J. Biomed. Opt. **11**, 024015 (2006)